OO -

dicted rms delay spread are 0.5 and 1.1 ns, respectively. The good agreement between our predicted and measured rms delay spread shows the validity of our model in predicting the various multipath components.

REFERENCES

1. S.Y. Tan and H.S. Tan, Improved three-dimensional ray tracing technique for microcellular propagation models, Electron Lett 31 (1995), 1503–1505.
2. S.Y. Seidel and T.S. Rappaport, Site-specific propagation prediction for wireless in-building personal communication system design, IEEE Trans Veh Technol 43 (1994), 879–891.
3. S.Y. Tan and H.S. Tan, Modelling and measurements of channel impulse response for an indoor wireless communications system, Proc Inst Elect Eng 142 (1995), 405–410.
4. K.R. Schaubach, N.J. Navis, and T.S. Rappaport, A ray tracing method for predicting path loss and delay spread in microcellular environments, Proc 42nd IEEE Veh Technol Conf, Denver, CO, vol. 2, pp. 932–995.
5. S.Y. Tan and H.S. Tan, A theory for propagation path loss characteristics in a city street-grid, IEEE Trans Electromag Compat 37 (1995), 333–342.
6. H.R. Anderson, Building corner diffraction measurements and predictions using UTD, IEEE Trans Antennas Propagat 46 (1998), 292–293.
7. C.D. Taylor, S.J. Gutierrez, S.L. Langdon, K.L. Murphy, and Walton, "Measurements of RF propagation into concrete structures over the frequency range 100 MHz to 3 GHz," Wireless personal communications, J.H. Reed, T.S. Rappaport, and B.D. Woerner (Editors), Kluwer Academic, Boston, MA, 1997, pp. 131–144.

FREQUENCY CHIRP ANALYSIS OF INJECTION-LOCKED SEMICONDUCTOR LASERS

Young-Kwang Seo[1] and Woo-Young Choi[1]
[1] Department of Electrical and Computer Engineering
Yonsei University
Seoul 120-749, Korea

Received 5 January 2000

ABSTRACT: *The chirping characteristics of an injection-locked semiconductor laser have been investigated. The frequency chirp of an injection-locked semiconductor laser has three contributions—dynamic, DC, and OIL chirp. It is greatly reduced since the OIL chirp is compatible to the DC and dynamic chirp, but different in sign.* © 2000 John Wiley & Sons, Inc. Microwave Opt Technol Lett 25: 374–377, 2000.

Key words: *injection locking; frequency chirp; strong optical injection; chirp reduction*

I. INTRODUCTION

In optical injection locking (OIL), the light from one laser (master laser, ML) is injected into another laser (slave laser, SL). The injected light causes changes in the SL characteristics, and it can lock the SL lasing frequency to the ML lasing frequency. The locking characteristics are determined by the amount of injected power and the frequency difference between the ML and SL.

OIL can greatly improve the semiconductor laser characteristics. It can reduce frequency chirp, linewidth, and noise [1, 2], enhance the modulation bandwidth [3, 4], and suppress the nonlinear distortion [5]. There have been several system demonstrations that utilize these improvements. Chirp-free digital transmission up to 10 Gbits/s was demonstrated by several research groups [7–9]. Meng et al. [10, 11] demonstrated the analog fiber-optic link in the frequency range beyond the intrinsic laser bandwidth, as well as the reduction of nonlinear distortions in the gigahertz range.

One of the key performance enhancements achieved with OIL is the reduction of frequency chirp. In this paper, the chirping characteristics of injection-locked semiconductors are analyzed. Based on the rate equation analysis, three factors that contribute to frequency chirping are identified, and their contributions are numerically analyzed. It is found that strong optical injection is desirable in order to maintain the SL in the stable-locking regime during large current modulation, and the contribution of the external light injection results in a significant chirp reduction.

II. ANALYSIS OF INJECTION-LOCKED SEMICONDUCTOR LASERS

In the OIL configuration, the CW light from the ML is injected into the SL. Two lasers have a frequency difference Δf defined as $f_{ML} - f_{SL}$. It is assumed in our analysis that the injected light has the same polarization as the SL lasing mode, which can be easily achieved with a polarization controller in reality. Assuming that DFB lasers with negligible side modes are used for both the ML and SL, the SL under the influence of external light injection can be described by the following single-mode rate equations [12]:

$$\frac{dP}{dt} = \left[\frac{\Gamma g_0}{1+\varepsilon P}(N-n_t) - \frac{1}{\tau_p}\right]P + \frac{\Gamma\beta}{\tau_n}N + 2K_C\sqrt{P_{in}P}\cos(\Phi_{ML}-\Phi) \quad (1)$$

$$\frac{d\Phi}{dt} = -2\pi\Delta f + \frac{1}{2}\alpha\left[\Gamma g_0(N-n_t) - \frac{1}{\tau_p}\right] + K_C\sqrt{\frac{P_{in}}{P}}\sin(\Phi_{ML}-\Phi) \quad (2)$$

$$\frac{dN}{dt} = \frac{I}{qV_a} - \frac{g_0}{1+\varepsilon P}(N-n_t)P - \frac{N}{\tau_n}. \quad (3)$$

In the above equations, P_{in} and Φ_{ML} represent the density and phase of the injected photons. Other parameters have the usual meanings, and their numerical values for the present analysis are obtained from [13] and listed in Table 1.

If the gain suppression and spontaneous emission (i.e., $\varepsilon = 0$ and $\beta = 0$) are ignored, the range of Δf that allows injection locking can be determined as [12]

$$|\Delta f(=f_{ML}-f_{SL})| \le \frac{K_C}{2\pi}\sqrt{\frac{P_{in}}{P}(1+\alpha^2)}. \quad (4)$$

This locking range can be further classified into two distinctive regimes: stable locking and unstable locking. In the stable-locking regime, the output power converges to a steady-state value when a small perturbation is introduced. In

TABLE 1 Parameter Values

Symbol	Parameter	Value
λ	Lasing wavelength	1550 [nm]
Γ	Confinement factor	0.4
n_t	Transparent carrier density	1.0×10^{18} [cm^{-3}]
τ_p	Photon lifetime	3.0×10^{-12} [s]
τ_n	Carrier lifetime	1.0×10^{-9} [s]
β	Spontaneous emission factor	3.0×10^{-5}
v_g	Group velocity	8.5×10^{9} [cm/s]
g_0	Differential gain	12.75×10^{-7} [cm^3/s]
ε	Gain suppression factor	5×10^{-17} [cm^3]
V_a	Volume of active layer	1.5×10^{-10} [cm^3]
α	Linewidth enhancement factor	5
η_{ex}	LD differential quantum efficiency	0.4
L_c	Active cavity length	300 [μm]
K_c	Coupling rate	$v_g/2L_c$

the unstable-locking regime, however, the power does not converge to the steady-state value, but experiences a self-sustained oscillation or even chaos when a small perturbation is introduced [12]. Such nonlinear behaviors are not desired, and our analysis is limited to the stable-locking regime.

The conditions for the stable-locking regime can be determined by the s-domain stability analysis of the linearized OIL rate equations. Figure 1 shows the upper and lower boundaries of Δf for stable locking as a function of SL bias currents for three different injected powers ($P_{inj} = 0.1$, 0.5, and 1 mW). As can be seen from the figure, the stable-locking range becomes narrower with increasing bias currents, but it widens with larger injected power. Hence, the strong optical injection is desirable for maintaining the SL in the stable-locking regime during large current modulation.

From Eq. (1) with the approximation of $g_0/(1 + \varepsilon P)$ by $g_0(1 - \varepsilon P)$,

$$\left[\Gamma g_0(N - n_t) - \frac{1}{\tau_p}\right] = \frac{1}{P}\frac{dP}{dt} + \Gamma g_0 \varepsilon (N + n_t)P$$
$$\frac{\Gamma \beta N}{\tau_n P} - 2K_C\sqrt{\frac{P_{in}}{P}}\cos(\Phi_M - \Phi). \quad (5)$$

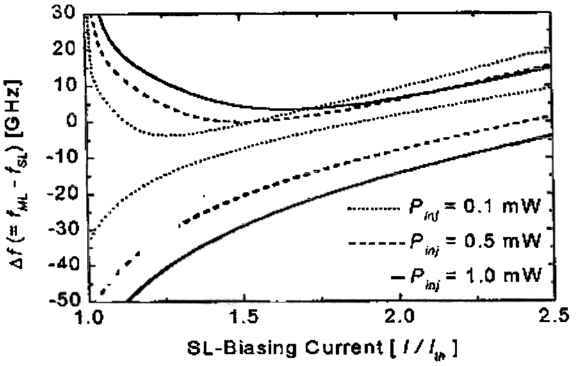

Figure 1 Dependence of the stable-locking range on the biasing current level

By substituting Eq. (5) into Eq. (2), Eq. (2) becomes

$$\frac{d\Phi}{dt} = \frac{1}{2}\alpha\left[\frac{1}{P}\frac{dP}{dt} + \Gamma g_0 \varepsilon (N - n_t)P - \frac{\Gamma\beta N}{\tau_n P} - 2K_C\sqrt{\frac{P_{in}}{P}}\cos(\Phi_M - \Phi)\right] - 2\pi\Delta f + K_C\sqrt{\frac{P_{in}}{P}}\sin(\Phi_{ML} - \Phi) \quad (6)$$

The frequency chirp δv is defined as $(1/2\pi)(d\Phi/dt)$, and it can be expressed as the sum of three factors:

$$\delta v = \delta v_{\text{dynamic}} + \delta v_{\text{DC}} + \delta v_{\text{OIL}} \quad (7)$$

where

$$\delta v_{\text{dynamic}} = \frac{\alpha}{4\pi}\frac{1}{P}\frac{dP}{dt} \quad (8)$$

$$\delta v_{\text{DC}} = \frac{\alpha}{4\pi}\left[\varepsilon\Gamma g_0(N - n_t)P - \frac{\beta\Gamma N}{\tau_n P}\right] \quad (9)$$

and

$$\delta v_{\text{OIL}} = -\Delta f - \frac{K_C}{2\pi}\sqrt{\frac{P_{in}}{P}}\,[\alpha\cos(\Phi_{ML} - \Phi) - \sin(\Phi_{ML} - \Phi)]. \quad (10)$$

The dynamic chirp is proportional to the rate of change in the SL photon density, and the DC chirp is the amount of the lasing frequency shift from a reference frequency. When the optical power increases, the dynamic and DC chirp show a positive sign. In contrast, the OIL chirp shows a negative sign.

III. NUMERICAL RESULTS AND DISCUSSION

In order to investigate the nature of chirp reduction with injection locking, the rate equations [Eqs. (1)–(3)] are numerically solved with the fourth-order Runge–Kutta integration method for a rectangular current pulse input of 0.5 ns duration, and each chirp contribution is identified. Φ_{ML} of 0 rad is used for the calculation. The SL-biasing and modulation current levels are assumed as $1.1 \times I_{th}$ and $1 \times I_{th}$, respectively. The frequency difference Δf is selected from Figure 1, at which the lasers are stable locked under the given modulation condition. The rise and fall times of a 25% pulse period are taken into account.

Figures 2 and 3 show the transient optical power (a) and frequency chirp (b) for the free-running and injection-locked ($P_{inj} = 1$ mW and $\Delta f = -12$ GHz) lasers. The current pulse is applied at $t = 0$. Figure 2 shows that the free-running laser undergoes relaxation oscillation, and has the combined effect of $\delta v_{\text{dynamic}}$ (dotted line) and δv_{Dc} (dashed line) during the modulation. The reference for the frequency shift is the lasing frequency at the threshold. Due to $\delta v_{\text{dynamic}}$, the lasing frequency shifts up when the output power rises, and shifts down when the output power fails. Due to δv_{DC}, the on state with larger photon and carrier densities has a larger chirp than the off state.

Injection-locked lasers, however, show quite different chirp characteristics, as can be seen in Figure 3. The reference for the frequency shift is the ML lasing frequency because the SL lasing frequency shifts to the ML's frequency. First of all, $\delta\upsilon_{dynamic}$ (dotted line) is reduced during the current modulation since the optical power fluctuates less, as noted in Figure 3(a). The reduction in optical power fluctuation is due to the suppression of relaxation oscillation by injection locking [14]. The major contribution to chirp reduction comes from $\delta\upsilon_{OIL}$ (dash–dotted line) that has a negative sign, as in Figure 3(b). Figure 3 shows that $\delta\upsilon_{OIL}$ drops when the output power rises. Since the magnitude of this negative chirp from $\delta\upsilon_{OIL}$ is nearly comparable to the positive chirp from $\delta\upsilon_{dynamic}$ and $\delta\upsilon_{DC}$, the injection-locked lasers show a small frequency chirp in the steady state.

Figure 4 shows another transient optical power and the corresponding frequency chirp for the injection-locked ($P_{inj} = 1$ mW) laser with a different value for Δf. At $\Delta f = 3.5$ GHz, the optical power fluctuates considerably, even in the on state. This is because the shift of Δf toward the upper boundary in Figure 1 causes less damping of the relaxation oscillation [14]. The influence of the fluctuating optical power on the frequency chirp is illustrated in Figure 4(b), where not only the dynamic chirp, but also the DC and corresponding OIL chirp oscillate in response to the optical power oscillation. However, the total frequency chirp is considerably reduced as well.

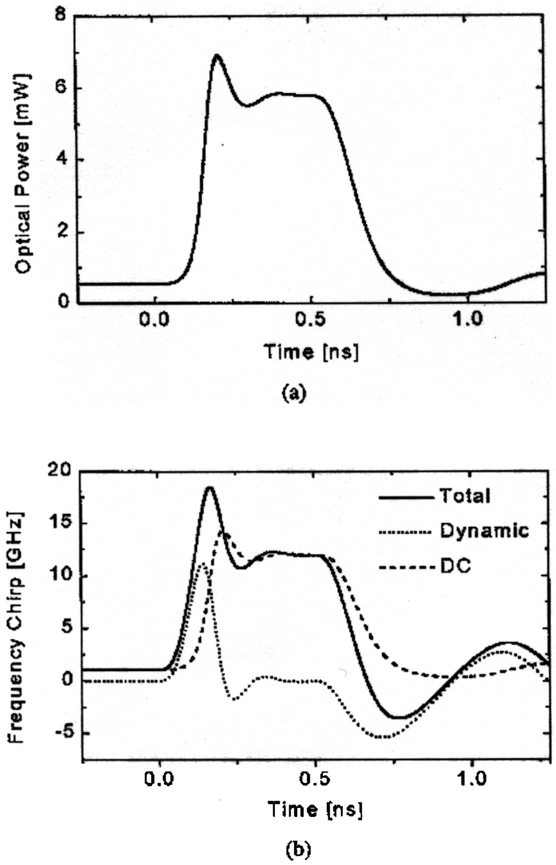

Figure 2 Transient optical power (a) and frequency chirp (b) for the free-running laser

IV. CONCLUSION

The chirping characteristics of an injection-locked semiconductor laser have been investigated. The frequency chirp of injection-locked semiconductor lasers has three contributions

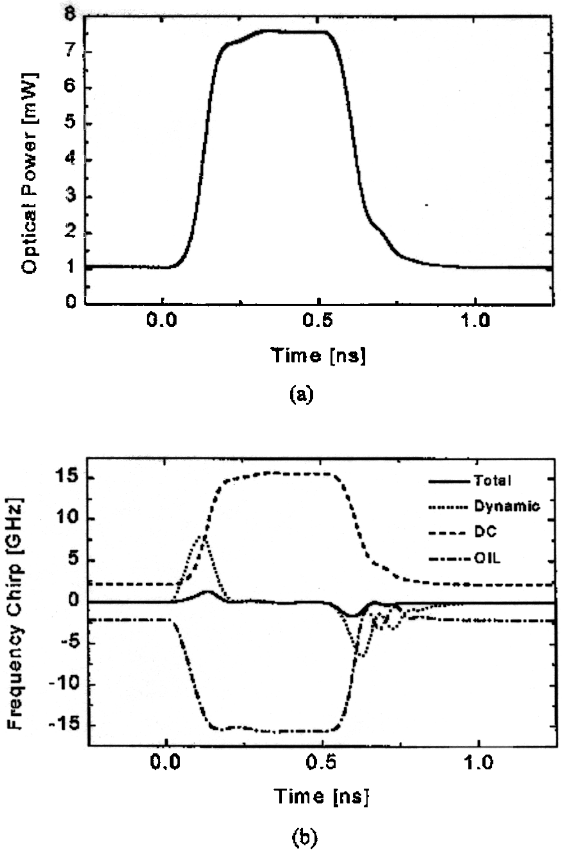

Figure 3 Transient optical power (a) and frequency chirp (b) for the injection-locked ($P_{inj} = 1$ mW and $\Delta f = -12$ GHz) lasers

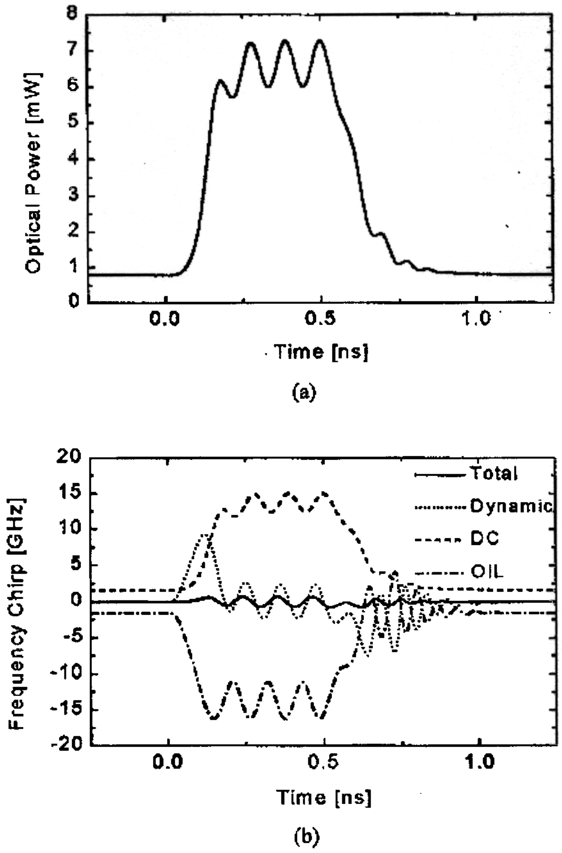

Figure 4 Transient optical power (a) and frequency chirp (b) for the injection-locked ($P_{inj} = 1$ mW and $\Delta f = 3.5$ GHz) lasers

—dynamic, DC, and OIL chirp. By numerically analyzing the rate equations for the injection-locked laser, it is shown that the OIL chirp is compatible to the DC and dynamic chirp, but different in sign. Hence, a considerable reduction in frequency chirp can be achieved by the OIL.

REFERENCES

1. C. Lin and F. Mengel, Reduction of frequency chirping and dynamic linewidth in high-speed directly modulated semiconductor lasers by injection locking, Electron Lett 20 (1984), 1073–1075.
2. M. Yoshno and K. Inoue, Chirp reduction in wavelength conversion using a laser diode by injection locking, Electron Lett 30 (1994), 1956–1957.
3. J.M. Liu, H.F. Chen, X.J. Meng, and T.B. Simpson, Modulation bandwidth, noise, and stability of a semiconductor laser subject to strong injection locking, IEEE Photon Technol Lett 9 (1997), 1325–1327.
4. G. Yabre, Effect of relatively strong light injection on the chirp-to-power ratio and the 3 dB bandwidth of directly modulated semiconductor lasers, J Lightwave Technol 14 (1996), 2367–2373.
5. J. Wang, M.K. Haldar, L. Li, and F.V.C. Mendis, Enhancement of modulation bandwidth of laser diodes by injection locking, IEEE Photon Technol Lett 8 (1996), 34–36.
6. G. Yabre and J.L. Biban, Reduction of nonlinear distortion in directly modulated semiconductor lasers by coherent light injection, IEEE J Quantum Electron 33 (1997), 1132–1140.
7. H. Toba, Y. Kobayashi, and K. Yanagimoto, Injection-locking technique applied to a 170 km transmission experiment at 445.8 Mbit/s, Electron Lett 20 (1984), 370–371.
8. N.A. Olsson, H. Temkin, R.A. Logan, L.F. Johnson, G.J. Dolan, J.P. Van der Zoel, and J.C. Campbell, Chirp-free transmission over 82.5 km of single mode fibers at 2 Gbit/s with injection locked DFB semiconductor lasers, J Lightwave Technol 3 (1985), 63–67.
9. S. Mohrdiek, H. Burkhard, and H. Walter, Chirp reduction of directly modulated semiconductor lasers at 10 Gb/s by strong CW light injection, J Lightwave Technol 12 (1994), 418–424.
10. X.J. Meng, D.T.K. Tong, T. Chau, and M.C. Wu, Demonstration of an analog fiber-optic link employing a directly modulated semiconductor laser with external light injection, IEEE Photon Technol Lett 10 (1998), 1620–1622.
11. X.J. Meng, T. Chau, and M.C. Wu, Improved intrinsic dynamic distortions in directly modulated semiconductor lasers by optical injection locking, IEEE Trans Microwave Theory Tech 47 (1999), 1172–1176.
12. J. Troger, P.-A. Nicati, L. Thevenaz, and Ph.A. Robert, Novel measurement scheme for injection-locking experiments, IEEE J Quantum Electron 35 (1999), 32–38.
13. J.C. Cartledge and G.S. Burley, The effect of laser chirping on lightwave system performance, J Lightwave Technol 7 (1989), 568–573.
14. I. Petitbon, P. Gallion, G. Debarge, and C. Chabran, Locking bandwidth and relaxation oscillations of an injection-locked semiconductor laser, IEEE J Quantum Electron 24 (1988), 148–154.

FREQUENCY OPTIMIZATION OF PSEUDOMORPHIC MODULATION-DOPED FIELD-EFFECT TRANSISTOR (AlGaAs/InGaAs) FOR MICROWAVE AND MILLIMETER-WAVE APPLICATIONS

Anju Agrawal,[1] Anisha Goswami,[2] and R. S. Gupta[2]
[1] Department of Electronics
Acharya Narendra Dev College
New Delhi 110 019, India
[2] Semiconductor Devices Research Laboratory
Department of Electronic Science
University of Delhi, South Campus
New Delhi 110 021, India

Received 2 November 1999

ABSTRACT: *The results of an analysis based on the solution of the 2-D Poisson equation are presented to investigate the dependence of the small-signal parameters on biasing conditions. The switching parameters are calculated simply from the charge variations, and it is found that the characteristics depend only on the basic device parameters and terminal voltages. The high value of f_t proves the utility of the model in the design of low-power MMICs. A maximum frequency of 101.42 GHz at 0.25 μm is obtained, and the results show close agreement with the experimental data, thereby proving the validity of the proposed model.* © 2000 John Wiley & Sons, Inc. Microwave Opt Technol Lett 25: 377–383, 2000.

Key words: *pseudomorphic MODFET; transconductance; drain conductance; cutoff frequency*

INTRODUCTION

The need for a higher frequency of operation in microwave and millimeter-wave applications and for very high-speed digital circuits in the gigabit range has created a great deal of interest in high-speed devices. The MODFET is a promising candidate for microwave, millimeter-wave, and digital circuits [1]. Applications presently being pursued in many laboratories include millimeter microwave integrated circuits, high-speed digital electronics for superconductors, and high-speed optoelectronics for gigabit fiber-optic communication.

As the gate length of a field-effect transistor is reduced to subquarter dimensions, the electron transit time across the gate region may become comparable to other time delays external to the intrinsic device [2, 3]. As a result, the key to realizing ultra-high-speed devices is to minimize not only the electron transit time, but also these extrinsic delays. The pseudomorphic AlGaAs/InGaAs (on GaAs) modulation-doped structures are among a few excellent candidates for such devices due to their high electron velocity, sheet density, and mobility, all of which are expected to help reduce the extrinsic delays associated with the parasitic capacitance and channel charging time.

The transconductance of the device is one of the most important indicators of device quality for microwave and millimeter-wave applications. These devices have shown a high value of 2-DEG concentration, and exhibit high 2-D electron mobility; hence, a higher value of transconductance is expected. The HEMT structure takes advantage of superior electron transport properties to provide high values of transconductance. Likewise, the carrier confinement obtained in the 2-DEG of an HEMT structure contributes to high output resistance. When all other characteristics are equal, a device with high transconductance will provide greater gains